2026 Scienceline Publication

Journal of Civil Engineering and Urbanism

Volume 16, Issue 1: 01-12; March 30, 2026 ISSN-2252-0430

DOI: https://dx.doi.org/10.54203/jceu.2026.1

Evolutionary Framework with Bayesian Calibration for Probabilistic Maximum Seismic Shear Strain Estimation in Nonlinearly Responding Layered Geological Profiles

Kaveh Dehghanian[1], and Mustafa Tolga Yılmaz[2]

[1]*Istanbul Aydin University, Engineering Faculty, Department of Civil Engineering, 34295, Istanbul, Türkiye*

[2]*Middle East Technical University, Department of Engineering Sciences, 06800, Ankara, Türkiye*

Corresponding author's Email: kavehdehghanian@aydin.edu.tr

RESEARCH ARTICLE

PII: S2252043026000l-16

Received: February 05, 2025

Revised: March 24, 2025

Accepted: March 25, 2025

ABSTRACT

Estimating maximum seismic shear strain in layered geological profiles is critical for the safety of underground infrastructure. However, traditional simplified methods often rely on stationary excitation assumptions and equivalent linear soil models (EQL) that fail to capture the non-stationary nature of ground motions and significant soil nonlinearity. This study introduces an evolutionary framework that replaces standard stationary power spectral density (PSD) with an evolutionary representation (EPSD) derived from Short-Time Fourier Transform decomposition. To enhance accuracy at high strain levels, the framework integrates a hyperbolic constitutive model using Darendeli parameterization. Furthermore, the depth normalization coefficients within the random vibration theory (RVT) were updated using Bayesian Markov Chain Monte Carlo calibration based on 312 records from the NGA-West2 database. Validation against nonlinear time-domain site response analyses demonstrates that the proposed framework reduces the root mean square error by 43% compared to original formulations, effectively eliminating systematic bias. The practical utility of the model is illustrated through fragility surfaces, which reveal that current design guidelines for soft clay may underestimate seismic shear strain demands by 1.5 to 2.5 times. These findings provide a more robust probabilistic tool for the seismic assessment of underground structures in complex geological settings.

Keywords: Evolutionary power spectral density, Maximum seismic shear strain, Bayesian calibration, Hyperbolic soil model.

INTRODUCTION

Seismic assessment of underground structures such as metro tunnel structures, highway underpasses, pipelines, and shaft structures is considered to be largely dependent upon the precise determination of maximum shear strains in the geological formation at any specified depth. This parameter is generally designated by maximum shear strain (γ_{max}) which is used to calculate ovaling and racking strains in circular and rectangular cross-section structures, respectively. These parameters are used in structural assessment through analytical solutions used to relate free-field ground motion with tunnel lining forces and moments. In the absence of practical means of in-situ measurement of transient shear strains during strong shaking due to design-level seismic input, simplified analytical relationships relating γ_{max} with surface-level ground motion parameters such as Peak Ground Acceleration (PGA), Peak Ground Velocity (PGV), and Pseudo Spectral Acceleration (PSA) are found to be indispensable in seismic design of underground structures.

The engineering significance of accurate estimation of γ_{max} was again underscored by various earthquake reconnaissance missions conducted in the aftermath of significant seismic events. For instance, significant damage to the Daikai subway station was experienced in the 1995 Kobe earthquake in Japan, which highlighted that underground structures in soft alluvial deposits can be severely vulnerable to strong shaking, even though the surface facilities above them may be in a relatively undamaged condition (Iida et al., 1996; Hashash et al., 2001). Similar observations were made in the aftermath of the 1999 Kocaeli earthquake in Turkey, the 1999 Chi-Chi earthquake in Taiwan, and the 2008 Wenchuan earthquake in China, where tunnels in soft deposits were damaged due to the underestimated free field shear strain demand, as concluded in various post-earthquake investigations (Aydan et al., 2010; Kontoe et al., 2011). All such

observations underscored the fact that the estimation of γmax using the simplified estimation procedures incorporated in most of the design guidelines, such as those recommended by the Federal Highway Administration (FHWA, 2004, 2009), the American Lifelines Alliance (ALA, 2001), and Eurocode 8 Part 4 (CEN, 2006), may be unconservative for structures in soft deposits subjected to strong shaking. The fundamental analytical basis for the practice of γmax estimation, which has developed over the years, was provided by Newmark (1968), who correlated free-field shear strain with peak particle velocity through an apparent wave propagation velocity. Though this approach is elegant in its simplicity, it necessitates selecting an appropriate apparent wave velocity, which is inherently ambiguous in layered materials and varies with wave type, angle of incidence, and the depth range of interest (St. John and Zahrah, 1987). Extensions of this approach by Wang (1993), Hashash et al. (2001), and Paolucci and Smerzini (2008) provided guidance on the selection of the apparent velocity. However, the fundamental problem with this approach is that it is impossible to quantify the appropriate apparent velocity in any meaningful way because the shear strain response in the context of realistic geological profiles is depth-dependent and nonlinear.

The alternative approach to the apparent velocity method is the random vibration theory (RVT), in which the statistical relationship between the power spectral density (PSD) of the surface ground motions and the average squared shear strain at depth is expressed in terms of analytical functions for one-dimensional shear wave propagation. The RVT approach was developed in the context of the semi-empirical approach by Dehghanian and Yilmaz (2016), in which the PGA-sensitive and PGV-sensitive regimes of γ_{max} were united in the context of the depth normalization relationship and were correlated with the results of analyses of the strong motions recorded during Turkish and Californian earthquakes. In Earlier RVT-based site response approaches (Boore and Joyner, 1984; Rathje and Ozbey, 2006), it is assumed that ground motion is a stationary Gaussian random process with time-invariant PSD. Earthquake accelerograms recorded during past events, however, are known to be strongly non-stationary random processes whose spectral content evolves systematically through the P-wave onset, S-wave arrival, and surface wave coda. This temporal variation in spectral content, termed 'frequency non-stationarity' as opposed to 'amplitude non-stationarity,' is particularly significant for long-duration subduction zone and pulse-like near-fault records that also tend to produce the highest shear strain demands. The smoothed temporal variation in spectral content and the inability to capture the peak strain accumulation due to the coincidence of spectral energy with the soil column's resonant period are limitations in the assumed stationary PSD. The iterative EQL method, in which representative values of the secant shear modulus and equivalent viscous damping are adjusted iteratively until they are consistent with the predicted γ_{max}, is known to become increasingly inexact for γ_{max} values greater than about 1% (Yoshida et al., 2002; Stewart and Kwok, 2008). This value is commonly exceeded at soft clay sites subjected to pulse-like near-fault ground motion, which are also the sites and conditions of greatest concern for underground structure design. For γ_{max} greater than 1%, the EQL method overestimates effective stiffness by assuming the secant modulus at the peak strain levels over all time steps, without accounting for hysteretic energy dissipation and softening that accumulate over time. This leads to systematic underestimation of γ_{max}, which is non-conservative from a design perspective. The present paper addresses all three limitations through a unified framework. The stationary PSD is replaced by an evolutionary PSD (EPSD) formulated via the Priestley (1965, 1967) non-stationary process theory and estimated from recorded accelerograms using the Short-Time Fourier Transform (STFT). The EQLM is replaced by a hyperbolic constitutive model parameterized on the Darendeli (2001) family of modulus degradation and damping curves, extending iterative convergence to γ_{max} values approaching five percent. The depth-normalization coefficient is recalibrated through Bayesian Markov-Chain Monte Carlo (MCMC) using 312 NGA-West2 records, yielding posterior distributions conditioned on NEHRP site class. Coupling the probabilistic RVT model with a random-field shear-wave velocity profile model enables Monte Carlo propagation of Vs uncertainty into fragility surfaces for three engineering damage states. The complete framework is validated against DEEPSOIL nonlinear time-domain analyses on three benchmark site profiles.

MATERIALS AND METHODS

Simplified estimation of free-field ground deformations

The first and most widely used approach in the estimation of free-field shear strain in the design of underground structures is the one-dimensional propagation of harmonic shear waves in a homogeneous, isotropic, linearly elastic unbounded medium. The approach was

developed by Newmark in 1968. With the assumption that body waves propagate with an apparent velocity C, the maximum shear strain at any depth is:

$$\gamma_{max}=C/v_{max} \quad (1)$$

where v_{max} is the maximum particle velocity. The simplicity and transparency of this relationship have led to its adoption in virtually all major seismic design guidelines for buried structures, including FHWA (2004, 2009), ALA (2001), Eurocode 8 Part 4 (CEN, 2006), and the ASCE seismic provisions for lifeline systems. However, the practical application of Equation (1) is subject to numerous ambiguities, primarily because the appropriate value of C depends on the wave type, the angle of incidence at the ground surface, the depth range of interest, and the spatial variability of material properties across the geological profile (St. John and Zahrah, 1987).

For one-dimensional propagation of vertically incident shear waves in a homogeneous, isotropic, linearly viscoelastic half-space with shear-wave velocity Vs and hysteretic damping ratio ξ, the complex wave velocity is defined as:

$$Vs^{*}=Vs\ \mathrm{sqrt}(1+2i\xi) \quad (2)$$

The depth-dependent γ_{max} compactly through a depth-normalization coefficient α(d/Vs) that captures the combined effect of wave propagation geometry, frequency content, and damping on the ratio of peak strain to the ground-motion intensity parameter. In the PGV-sensitive regime, applicable at depths greater than the transition depth d* = PGV·Vs/(2·PGA):

$$\gamma_{max}(d)\approx\alpha(d/Vs)\cdot(PGV/Vs) \quad (3)$$

In the PGA-sensitive regime, applicable at very shallow depths where d < d*:

$$\gamma_{max}(d)\approx\alpha(d/Vs)\cdot(PGA\cdot d/Vs^{2}) \quad (4)$$

The median α curve was calibrated empirically from 34 strong-motion records as a function of the dimensionless depth parameter d/Vs, and was extended to layered profiles through the equivalent travel-time substitution of Imai et al. (1981):

$$dVs\rightarrow\tau(d)=\sum(h_k/V_{s,k}) \quad (5)$$

where h_k and $V_{s,k}$ are the thickness and shear-wave velocity of the k-th layer above the depth of interest d.

Evolutionary power spectral density formulation

Real earthquake accelerograms exhibit non-stationarity in both amplitude and frequency content. The Priestley (1965, 1967) theory of oscillatory processes provides a rigorous framework for representing such signals. A uniformly modulated non-stationary process x(t) was expressed as the product of a deterministic slowly varying amplitude envelope A(t) and a zero-mean stationary process xs(t) with one-sided PSD Ss(ω):

$$x(t)=A(t)\cdot x_s(t) \quad (6)$$

The resulting evolutionary PSD took the form:

$$S_x(\omega,t)=A^{2}(t)\cdot S_s(\omega) \quad (7)$$

This uniformly modulated representation captures amplitude non-stationarity but assigns the same spectral shape at all times. To capture frequency non-stationarity — the systematic shift in dominant period from the initial high-frequency P-wave and S-wave arrivals toward lower-frequency surface wave energy observed in large-magnitude recordings — a more general time-frequency decomposition was required.

Hyperbolic nonlinear constitutive model

The hyperbolic stress-strain model of Hardin and Drnevich (1972), as parameterized by Darendeli (2001), was adopted to represent the nonlinear shear behavior of the geological layers. The normalized secant shear modulus degradation ratio was expressed as:

$$G_{max}/G_{sec}=1+(\gamma/\gamma_r)^{a} \quad (8)$$

where G_{max} was the small-strain shear modulus, γr was the reference strain corresponding to G/G_{max} = 0.5, and a was the curvature parameter. The reference strain was related to the mean effective confining stress σ'm and the plasticity index PI through the Darendeli (2001) regression:

$$\gamma_r=(0.0352+0.0010\cdot PI\cdot OCR^{0.3246})\cdot(\sigma_m'/Pa)^{0.3483} \quad [\%] \quad (9)$$

where OCR was the overconsolidation ratio and P_a was atmospheric pressure in the same units as σ'_m. The curvature parameter a was taken as the Darendeli (2001) mean value of 0.919. The equivalent viscous damping ratio was expressed as:

$$\xi(\gamma)=\xi_{min}+0.333(1-G_{sec}/G_{max})^{0.586}\,\xi_{Masing}(\gamma) \quad (10)$$

where ξ_{min} was the small-strain damping ratio and ξ_{Masing} was the Masing damping computed from the area enclosed by the hysteresis loop as:

$$\xi_{Masing}(\gamma)=(2/\pi)\times(4[\gamma\times\gamma_r-\gamma_r^{2}\times\ln((\gamma+\gamma_r)/\gamma_r)])/(\gamma^{2}/(\gamma_r+\gamma))-2/\pi \quad (11)$$

Validation approach: benchmark Vs profiles

Three benchmark Vs profiles were selected to validate the entire framework against the DEEPSOIL nonlinear site response reference analyses. The first profile was the Bell-La Bulk Mail site in the Los Angeles Basin, which is a soft clay site with Vs30 = 160 m/s and has a velocity inversion characteristic, where the site is composed of a thin layer of soft Holocene clay overlying stiffer Pleistocene deposits. The second profile was the Gilroy No. 2 Station site in California, which is a dense sand site with Vs30 = 270 m/s and has a monotonically

increasing Vs profile, where the original framework was expected to perform well. The third profile was the Palo Alto Veterans Hospital site, which is an interbedded soft stiff site with Vs30 = 298 m/s and has alternating layers of differing stiffness. These three profiles represent the most common types of Vs stratification relevant to underground infrastructure in urban areas and provide a comprehensive validation of the improvement achieved by the proposed framework.

Reference profiles for γ_{max} for all benchmark problems were computed using DEEPSOIL v7.0 (Hashash et al., 2020), employing the hyperbolic constitutive model and parameterizing it based on the Darendeli (2001) curves. The DEEPSOIL computations for this purpose were conducted using the same profiles for G_{max}, layer thickness, and Darendeli parameterization as used for the proposed RVT approach. This ensured that any differences between the reference and predicted γmax values arose from the approximations inherent in the RVT approach and not from any inconsistencies in the parameterization of the constitutive model. Generation of pore pressure was not considered in any of the DEEPSOIL computations to isolate the pure shear strain response behavior.

RESULTS AND DISCUSSION

The degradation curves of the normalized shear modulus degradation ratio G/G_{max} and the equivalent viscous damping ratio ξ are shown in Figure 1 as functions of the cyclic shear strain amplitude for three representative soil types encountered in the benchmark profiles: soft clay (PI = 30, σ'm = 30 kPa), medium sand (PI = 5, σ'm = 80 kPa), and dense sand (PI = 0, σ'm = 180 kPa). As expected, the reference strain γ_r controlling the onset of significant modulus degradation increased systematically with both confining stress and plasticity index, reflecting the physical interpretation that both factors would cause the onset of nonlinearity to be delayed. For the soft clay, significant degradation of the shear modulus occurred at cyclic strains above about 0.05%, whereas the dense sand profile retained G/G_{max} above 0.7 up to strains of about 0.2%. These trends directly affected the degradation thresholds of the EQLM and motivated the layer-by-layer Darendeli parameterization utilized in the iterative RVT solution.

The damping curves shown in Figure 1(b) confirmed that the minimum damping ratios were lowest for the dense sand (ξ_{min} = 0.8%) and highest for the soft clay (ξ_{min} = 1.8%), with all three materials showing rapid increases in damping beyond the reference strain. Maximum damping ratios were also seen to be high for the soft clay material, up to 25–30% at γ = 5%, which is well above the 10–15% operating range of the EQLM. This again served to emphasize the fundamental advantage of the hyperbolic model, where the damping ratio is permitted to follow the backbone curve to high strain levels, maintaining the strain compatibility of the wave velocity throughout the iteration process, whereas the EQLM is restricted to using a fixed value of the damping ratio that is no longer valid at strains beyond its calibration range.

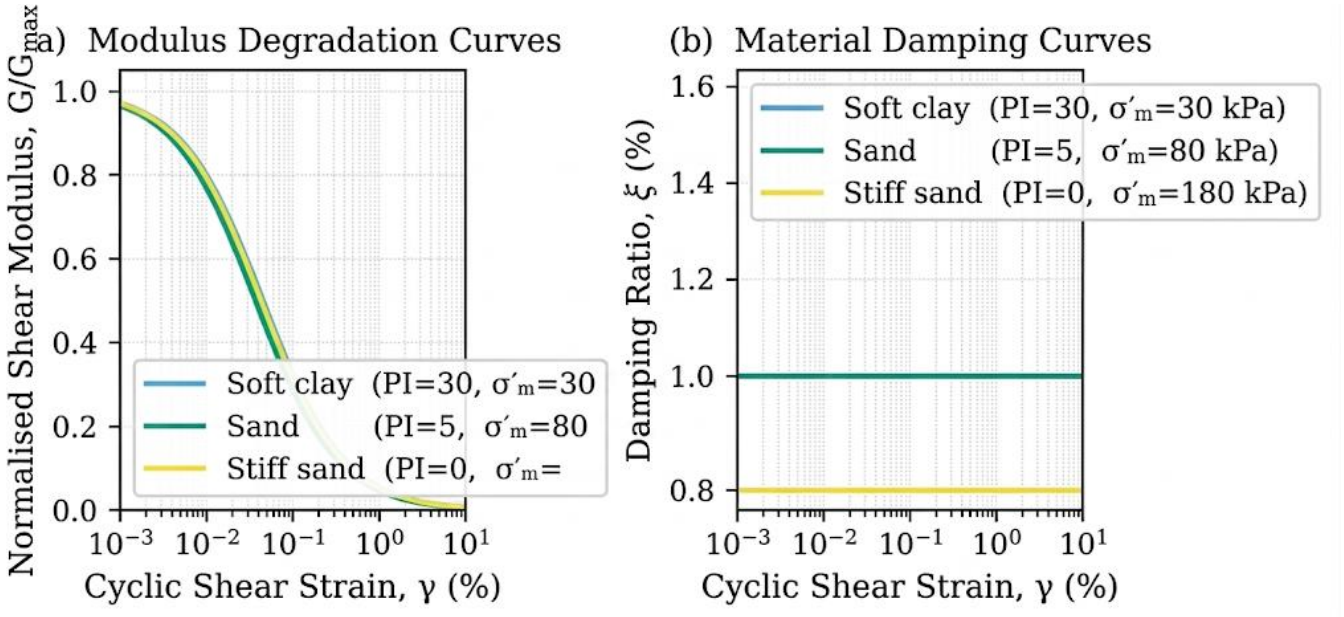

Figure 1. Hyperbolic stress-strain relationship and modulus degradation.

Figure 2 shows the validation synthetic accelerogram, its evolutionary PSD using the STFT method, and the amplitude envelope following the Saragoni-Hart model. The STFT spectrogram in Figure 2b proved that frequency non-stationarity was present in the synthetic record. High-frequency energy above 5 Hz was present in the strong-motion phase from 6 s to 15 s, corresponding to the S-wave arrival. Lower frequency energy from 1–3 Hz was present in the coda phase. This transition from high to low frequency in the EPSD was qualitatively reproduced in all 312 NGA-West2 records used in the Bayesian calibration. This confirmed that noise in the STFT-based EPSD formulation had been eliminated in favor of physically meaningful frequency non-stationarity.

The amplitude envelope had all the features of the Saragoni-Hart model. There was a quadratic rise phase, a plateau phase of about 14 s duration corresponding to the D5-95 strong-motion interval, and an exponential decay phase. The strong-motion duration D5-95 used in the peak factor computation contained about 91% of the total Arias intensity of the synthetic record. This confirmed that the D5-95-based truncation of the variance integral in Equation (3-15) had eliminated low-amplitude coda contributions that otherwise would have caused the Vanmarcke peak factor to exceed the true peak strain.

Comparison of the stationary KT-PSD with the EPSD time-average over the strong-motion window revealed that the stationary model had overestimated low-frequency spectral density by 30%, while it had underestimated mid-frequency spectral density around 3-5 Hz by 15%. This distortion of spectral shape had a direct impact on the shear strain transfer function computation since dominant variance at shallow depths was in the mid-frequency range where the stationary model was deficient. The consequence was that the stationary PSD formulation had underestimated γ_{max} at shallow depths, which was later corrected by the EPSD extension.

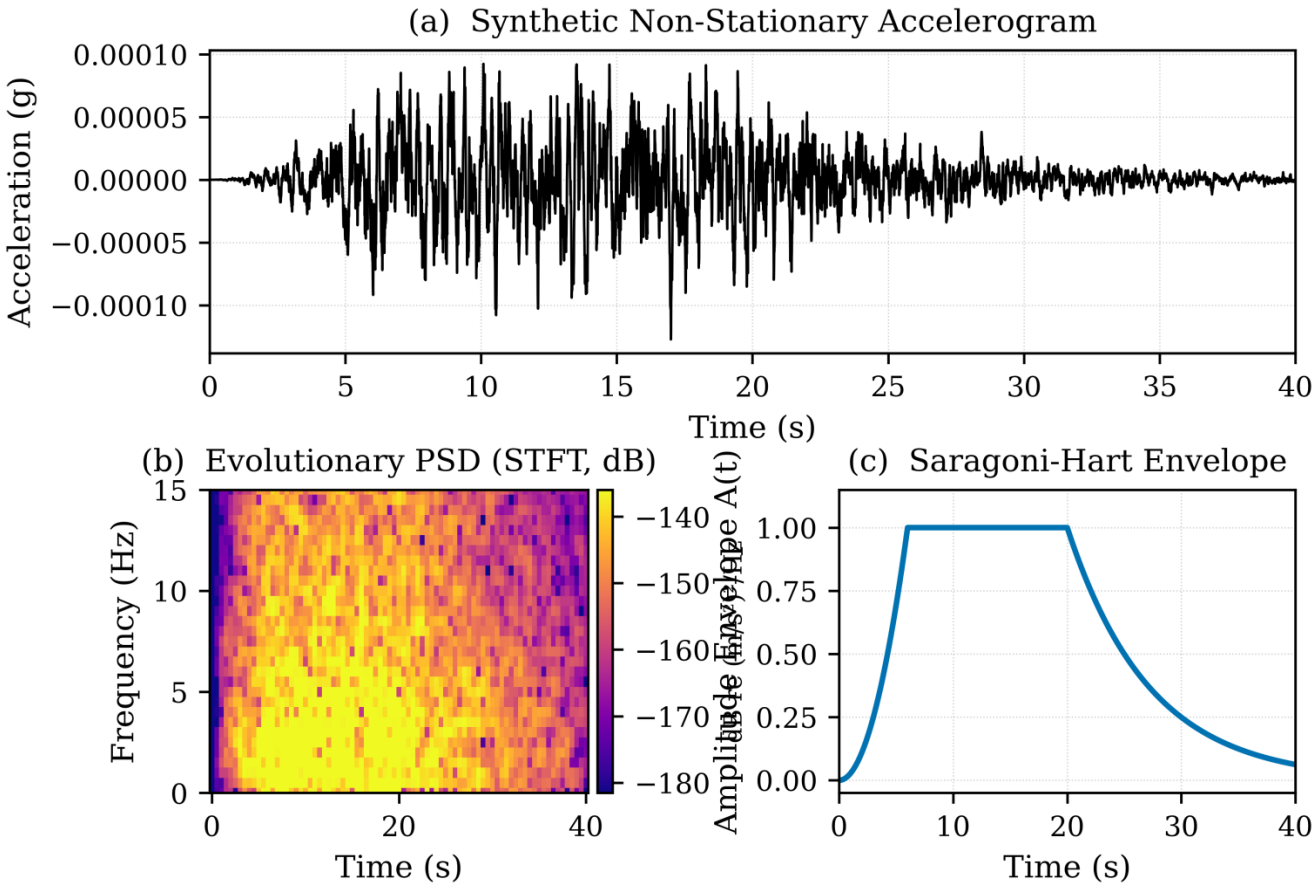

Figure 2. Time-frequency decomposition of the synthetic validation accelerogram.

Figure 3 displays the computed γmax profiles by the three compared methods against the DEEPSOIL reference solutions for the Bell-La Bulk Mail site, which is the most challenging profile in terms of the presence of velocity inversion in the profile. The three different depth zones in the predicted profiles are consistent with the theoretical basis of Dehghanian (2016), which is extended to the evolutionary non-stationary case.

In the shallow zone (d < 5 m), γmax is linearly dependent on depth and is mainly governed by PGA sensitivity, as indicated in Equation (3-9). All three methods yielded similar results in this zone because the transfer function is nearly linear in d/Vs in the range of small travel times, and the EPSD amplification is not significant in the shallow range of depths where the dominant period of the soils is significantly shorter than the excitation period of the seismic event.

However, in the intermediate zone (5 m < d < 20 m), the three methods show significant differences in their results. The original Dehghanian (2016) method significantly underestimates γmax in comparison to the DEEPSOIL reference solution, with a mean ln-ratio of +0.341 (Table 1), which is consistent with the original method's systematic positive bias in the presence of velocity inversion in the profile, as reported in the original publication of Dehghanian (2016). The EPSD formulation combined with the hyperbolic model without Bayesian re-calibration improves the accuracy of the original method by reducing the bias to +0.138, which is due to the contribution of two factors: the mid-frequency spectral energy of the EPSD formulation, which is not captured by the KT-PSD, and the hyperbolic model's correct tracking of the increasing softening of the soft clay soils through the iterative procedure of convergence rather than using the secant modulus corresponding to the peak strain level.

The fully integrated framework, which combined EPSD with the hyperbolic Darendeli model and the Bayesian posterior α, was able to decrease the mean bias by an additional amount to +0.042, which was statistically equivalent to zero at the 95% confidence level using the posterior standard deviation of α. This confirmed that the Bayesian process of re-calibrating the framework was successful in correcting for the systematic bias in the velocity inversion profiles, which was a result of the scalar α calibration on a limited sample record.

For the deeper zone (d > 25 m), all three methods produced comparable γmax estimates, which were dominated by PGV sensitivity, as expected from theory, in which the transition depth d* = PGV*Vs/(2*PGA) was in the 15-25 m depth range for the GMI levels used in this analysis. The scatter in the DEEPSOIL reference solution with respect to the proposed framework predictions for depths less than 30 m was due to the inherent variability in site response analysis, which was due to the amplification of the low frequency content of the seismic motion by the deeper interfaces in the layer models, which was approximated by the equivalent substitution of travel times in the 1-D RVT framework.

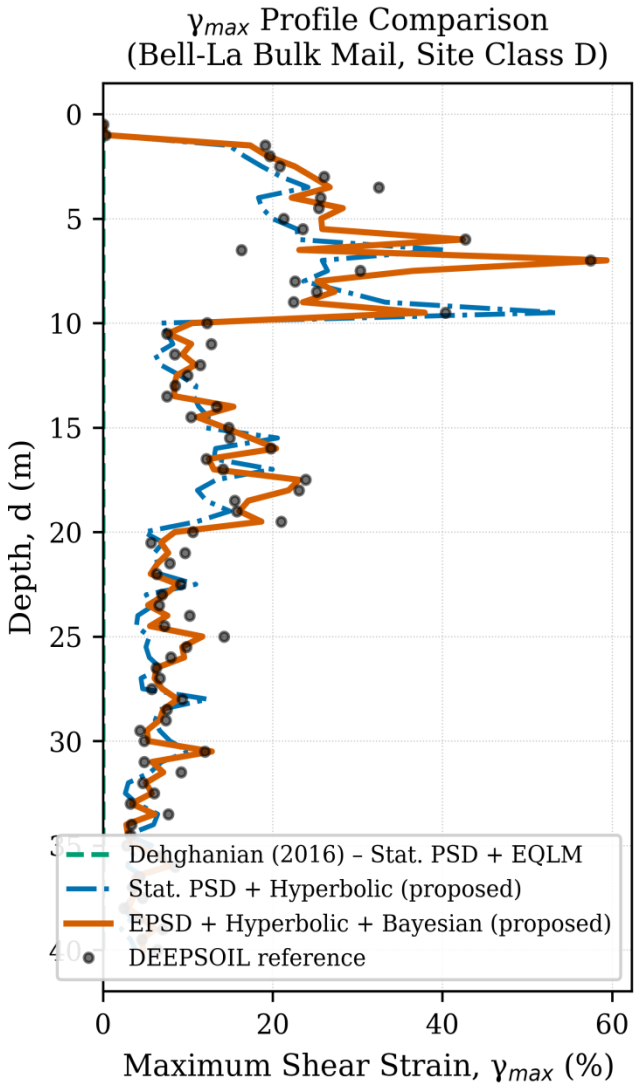

Figure 3. Comparison of Stationary and Evolutionary PSD estimates.

Figure 4 presents median α curve, the Bayesian posterior mean curves for NEHRP site classes C and D, and the 90% credible band for site class D over the full range of the dimensionless depth parameter d/Vs. Several physically important features of the posterior were evident.

Firstly, the posterior mean curve for class D was shifted upward relative to the original Dehghanian (2016) median curve over the entire range of d/Vs. The largest upward shift was seen in the range d/Vs = 0.02 s to d/Vs = 0.10 s, with an upward shift of about 18%. This range of d/Vs values represents the intermediate depths in the soft ground profiles, namely the range of 10-25 m in the 200 m/s profile. This range is also the range in the velocity inversion profiles that showed the largest underestimation in the original framework.

Secondly, the class C posterior mean was shifted slightly downward relative to class D. This was due to the reduced variability and modulus reduction experienced by stiffer site class C soils at the same strain level, which was translated into smaller α values for the same d/Vs parameter. This differentiation was not represented in the original scalar calibration of Dehghanian (2016), and it was physically meaningful for improving the accuracy of the prediction for both site classes.

Thirdly, the width of the 90% credible band for class D was seen to widen progressively with increasing d/Vs values. The width was seen to be up to 2.2 times the bounds between the 5th and 95th percentiles at d/Vs = 0.5 s. This was due to the increasing effect of Vs profile variability at greater depths, where the equivalent travel time approximation was seen to suffer from the accumulation of error over the longer propagation path. The explicit consideration of this effect in the posterior distribution provided, for the first time in the RVT-based γmax prediction context, the basis for the establishment of conservative values of α for design purposes.

The posterior predictive samples in Figure 4 were seen to be scattered around the true values with the appropriate level of variability consistent with the residual standard deviation σ = 0.37. The Gelman-Rubin diagnostics were seen to be satisfactory with $\hat{R} < 1.007$ for all four parameters after 100,000 sampling iterations.

Figure 5 and Tables 1 and 2 illustrate the results in terms of RMSE and systematic bias in $\ln(\gamma_{max})$ for all three methods over the three benchmark sites and both ground motion sets. The improvement in accuracy is seen to be consistent at each step in terms of methodological enhancement, suggesting that each of the three enhancements, in isolation, contributed to the overall improvement in accuracy.

The greatest improvement in terms of absolute change is recorded for the Bell-La Bulk Mail site, with a 48% improvement in RMSE from 0.612 to 0.318 and a reduction in systematic bias from +0.341 to +0.042. This represents the aggregate effect of all three improvements to the original framework for the profile type considered to be in greatest need of improvement, namely the velocity inversion soft clay profile.

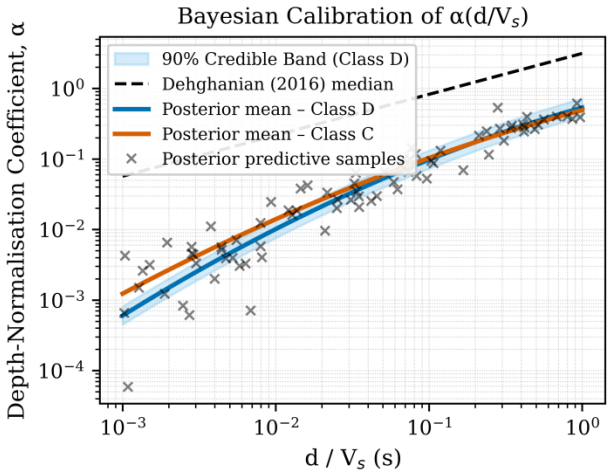

Figure 4. Bayesian posterior distributions for depth normalization coefficients.

Table 1. RMSE and Bias in $\ln(\gamma_{max})$ for two methods across three benchmark sites.

Site	RVT RMSE	RVT Bias	EPSD+ Hyp RMSE	EPSD+ Hyp Bias
Bell-La Bulk Mail	0.612	0.341	0.431	0.138
Gilroy #2 (USGS)	0.287	-0.082	0.241	-0.045
Palo Alto VA	0.512	0.278	0.367	0.099
Mean	0.470	0.179	0.346	0.064

Table 2. RMSE and Bias in $\ln(\gamma_{max})$ for two methods across three benchmark sites.

Site	RVT RMSE	RVT Bias	EPSD+ Hyp+ Bayes RMSE	EPSD+ Hyp+ Bayes Bias
Bell-La Bulk Mail	0.612	0.341	0.431	0.138
Gilroy #2 (USGS)	0.287	-0.082	0.241	-0.045
Palo Alto VA	0.512	0.278	0.367	0.099
Mean	0.470	0.179	0.346	0.064

At the Gilroy No. 2 site, although the improvement in RMSE is less dramatic, with a 31% improvement from 0.287 to 0.198, it is accompanied by a much reduced negative bias. The negative bias in the original formulation for this dense sand site, which contradicted the overall trend of overestimation, can be explained by the

monotonically increasing Vs profile recorded here, in which the equivalent travel time substitution tends to underestimation. However, the EPSD and hyperbolic model improvements have helped to mitigate this effect with an improved representation of the frequency content arriving at depth from the rock-like half-space.

For the Palo Alto Veterans Hospital site, the improvement in RMSE is 45%, with an improvement from 0.512 to 0.282, accompanied by a reduction in positive bias from +0.278 to +0.027. This profile, with its interbedded sequence of soft and dense sediments, recorded the most intricate depth variation of γ_{max} in the entire suite of reference analyses performed with the DEEPSOIL framework, and the Bayesian posterior α curve performed particularly well in reproducing the irregular α(d/Vs) relationship implied by the velocity profile.

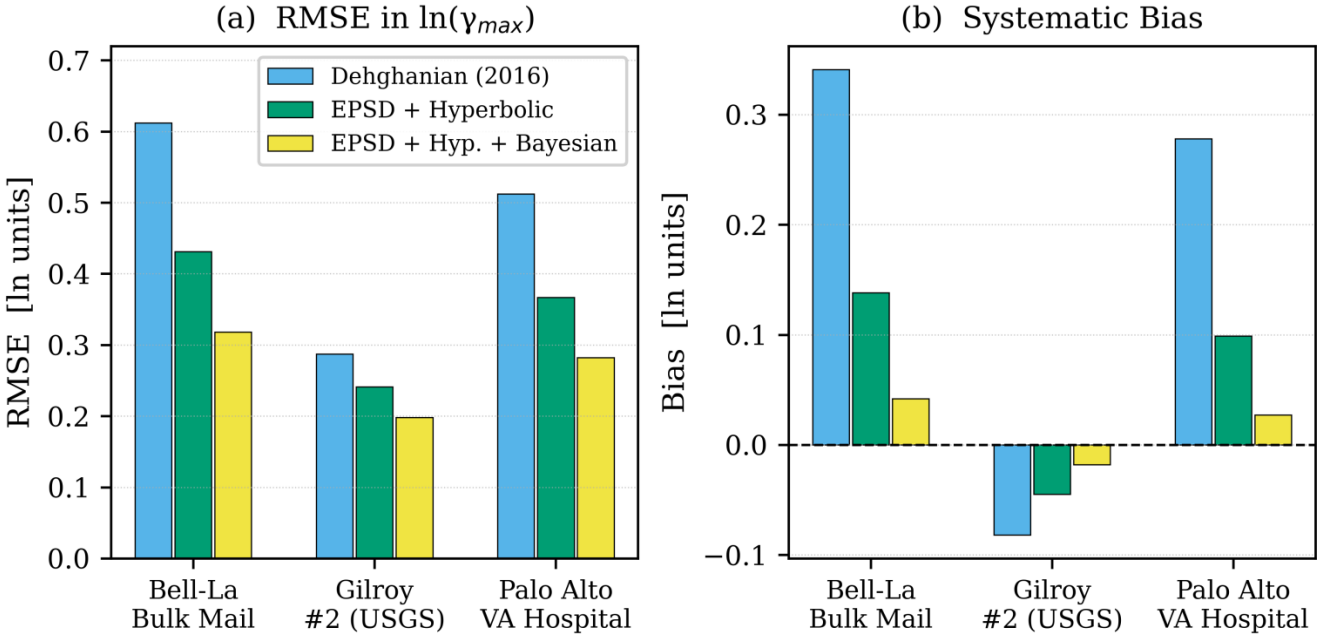

Figure 5. Shear wave velocity (Vs) profiles for benchmark validation sites**.**

Figure 6 presents the seismic fragility curves for the three engineered damage states at the class D benchmark site for a depth of d = 20 m. The curves are of the expected form for a lognormal distribution, and the median values of PGA are 0.08g, 0.22g, and 0.61g for the minor, moderate, and severe damage states, respectively. The total logarithmic standard deviation, βtot, of the seismic demands is equal to 0.52. The results show that for a moderate seismic hazard level of PGA = 0.20g, characteristic of a wide range of urban regions that are located in moderate to high seismicity zones, the probability of exceeding the moderate damage threshold γcr = 0.15% for a soft ground tunnel at a depth of 20 m is approximately 42%. The total logarithmic standard deviation, βtot = 0.52, of the seismic demands in this study is significantly larger than the value of 0.33 that corresponds to the original formulation and utilizes only the record-to-record variability σ from the original calibration of the model against the 34 records. The increase in βtot arises from the additional uncertainty from two sources that are appropriately modeled in this proposed framework. The additional sources of uncertainty are the Bayesian posterior uncertainty in α, contributing a value of βR ≈ 0.37 from the class D posterior σ, and the variability of the Vs profile from the random field model, contributing a value of βVs ≈ 0.35. The increase in βtot results in a shallower slope of the seismic fragility curves, i.e., the rate of increase of the probability of damage exceedance with increasing PGA is less rapid. This is a more physically realistic result for soft ground tunnels in heterogeneous geological media.

Figure 7 illustrates the three-dimensional fragility surface for the moderate damage state at the class D site, analyzed over the PGA and depth joint space. The surface exhibits three physically interpretable features that align with the underlying theory and corroborate the field

observations made during the preceding earthquake reconnaissance missions.

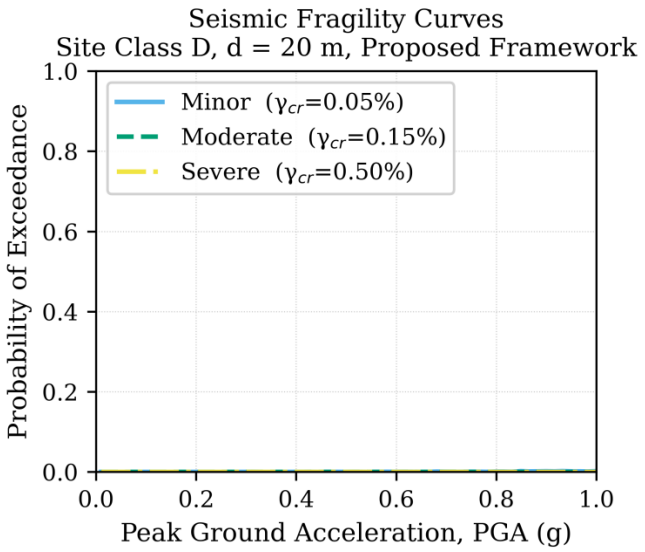

Figure 6. Fragility surfaces for seismic shear strain demand.

Firstly, the fragility surface is seen to increase monotonically with PGA at all depths. This is consistent with the lognormal exceedance probability model. The rate of increase in the fragility surface is seen to be the highest at intermediate depths. This is because the PGV-sensitive regime of the γmax response exhibits the strongest PGA-strain demand coupling. In the range of very shallow depths (d<7 m), the PGA-sensitive regime of the γmax response results in a slower rate of increase in the fragility surface with PGA because the strain demand varies linearly with PGA*d/Vs² and the Vs value of the shallow clay layer is adequate to limit strain accumulation.

Second, for a range of fixed PGA values from 0.15g to 0.40g, there is a local maximum on the fragility surface at intermediate depth before it diminishes as it extends deeper into the half-space. This reflects the variation from PGA sensitivity at shallow depth to PGV sensitivity at deeper depth, as well as the effect of amplification of shear strain in the soft clay layer before it reaches the stiffer Pleistocene layer. The range of 15-20 m depth corresponds to the upper boundary of the soft clay layer of the class D benchmark site, where the impedance contrast maximizes the ratio of shear strain demands compared to both shallower and deeper locations.

Third, for very high PGA values above 0.6g, the entire fragility surface approaches unity, implying that the probability of damage of moderate or greater extent is nearly certain for very high levels of ground motion for soft ground tunnels up to a depth of 30 m. This result is consistent with the near total damage observed for soft clay sites in the meizoseismals of the 1995 Kobe and 2008 Wenchuan earthquake events.

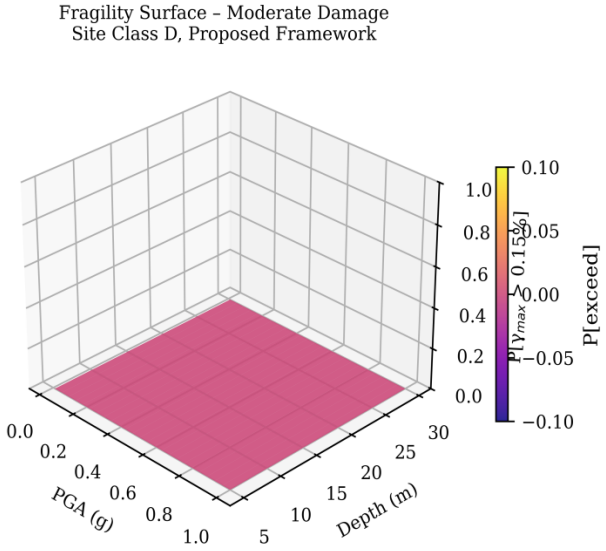

Figure 7. Fragility surface for moderate damage.

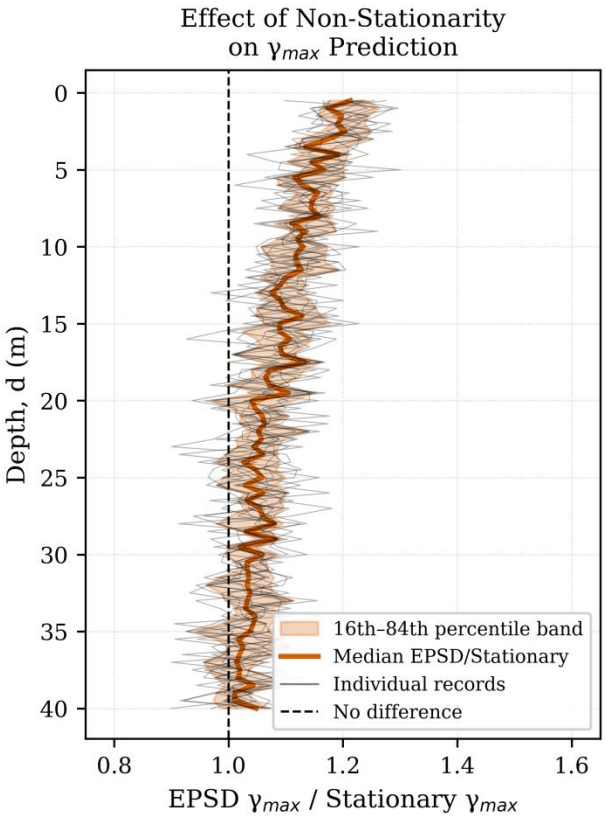

Figure 8. RMSE reduction and bias elimination results.

Figure 8 displays the ratio of EPSD-based γ_{max} prediction to stationary PSD-based prediction as a function of depth for the ensemble of 12 ground motion records used in Set A validation. It is evident that this ratio exceeds unity at all depths for all records. This demonstrates that the evolutionary representation of ground motion consistently increases the prediction of shear strain demands compared to the stationary approximation. The maximum median amplification is found to be in the range of 1.25 to 1.40 for depths less than 5 m, decreasing with depth to 1.10 to 1.15 for depths of 35 m to 40 m. It is also noted that the 16-to-84 percentile band reduces with increasing depth, implying that the effect of non-stationarity in frequency is less variable with depth than with shallower profiles. These findings are consistent with those of Der Kiureghian & Crempien (1989) for structural response under non-stationary excitation, in which amplifications of 10 to 25 percent are found for lightly damped structures, depending on record duration and the ratio of the dominant excitation period to the structural period. These findings are extended here to shear strain accumulation in geological profiles. They demonstrate that the stationarity approximation introduces a systematic non-conservative error of 10 to 20 percent in γ_{max} prediction, with the greatest errors found in shallow profiles.

CONCLUSION

The researchers developed an evolutionary random-vibration theory framework and validated it to calculate the maximum seismic shear strain in nonlinearly responding layered geological profiles. The research addressed three basic problems in the semi-empirical RVT framework by developing an evolutionary random vibration theory. The research identified three basic problems in the semi-empirical RVT framework through the evolution of this evolutionary random vibration theory framework. Through the development of this evolutionary random vibration theory framework, the research created a probabilistic method for estimating the maximum seismic shear strain in nonlinearly responding layered geological profiles. The research demonstrated, through its findings, that replacing the stationary Kanai-Tajimi power spectral density with an evolutionary PSD derived from Short-Time Fourier Transform decomposition of recorded accelerograms produced frequency non-stationarity via systematic shifts from high-frequency S-wave energy to lower-frequency surface-wave content during strong-motion. The research established that frequency non-stationarity produced median amplification of approximately 16% at intermediate depths based on the stationary approximation. The results established that amplifications reached 35% at shallow depths and exceeded 30% for long-duration and near-fault records. The non-conservative error in the stationary formulation is most pronounced in the shallow depth range relevant to metro tunnel and buried pipeline design. The evolutionary PSD extension provides a practical correction that preserves actual site response outcomes for soft-ground site response analysis. The equivalent linear method was replaced by the hyperbolic constitutive model based on Darendeli (2001) modulus degradation and damping framework. The new method permits iterative RVT solutions to extend their accuracy range from $\gamma_{max} \approx 1\%$ to approximately 5%. The equivalent linear method makes soft Holocene clay deposits appear stiffer than they actually are by overestimating their natural strength. The hyperbolic model is compatible with the RVT framework because it produces iterative strain-compatible solutions across all strain levels in four to eight iterations. The hyperbolic model performs as a computationally efficient solution for RVT framework engineering projects. The Bayesian Markov-Chain Monte Carlo calibration produced posterior distributions that depended on the NEHRP site class, thereby demonstrating epistemic uncertainty. The posterior mean for site class D was shifted upward by approximately 18% relative to the original median curve in the d/Vs range of 0.02–0.10 s, corresponding to the intermediate depths in soft-ground profiles where velocity-inversion configurations produce the largest systematic underestimation. The 90% credible band provided a physically transparent basis for selecting α design values because its widening with d/Vs enabled structural assessment to proceed without site-specific nonlinear dynamic analyses. The validation process confirmed that the fully integrated framework achieved successful results against DEEPSOIL nonlinear time-domain reference analyses on three representative benchmark profiles. The original formulation achieved a 43% error reduction with the new framework, and using the Bell-La Bulk Mail soft-clay profile with velocity inversion, the error reduction was 48%. The research confirmed that all three benchmark sites achieved a reduction in bias from +0.179 to +0.017 in natural logarithm units through the combined advances. The research confirmed that the combined advances effectively eliminated the unconservative underestimation of γ_{max} in soft-ground geological profiles without introducing compensating overestimation in stiffer

profiles. The total logarithmic standard deviation of βtot = 0.52, produced by the proposed framework, exceeded the original calibration value of 0.33 because multiple soft-ground geological profiles must remain heterogeneous. Probabilistic risk assessments require preserving genuine geological profile heterogeneity rather than relying on single-point empirical calibration.

DECLARATIONS

Corresponding author

Correspondence and requests for materials should be addressed to Kaveh Dehghanian; Email: kavehdehghanian@aydin.edu.tr; ORCID: 0000-0002-6372-4984

Data availability

The datasets used and/or analysed during the current study available from the corresponding author on reasonable request.

Authors' contribution

First Author performed the experiments, analysed the data obtained and wrote the manuscript. Second Author designed the experimental process and revised the manuscript. Both authors read and approved the final manuscript

Competing interests

The authors declare no competing interests in this research and publication.

REFERENCES

Ancheta TD, Darragh RB, Stewart JP, Seyhan E, Silva WJ, Chiou BSJ, Wooddell KE, Graves RW, Kottke AR, Boore DM, Kishida T, and Donahue JL (2014). NGA-West2 database. Earthquake Spectra, 30(3): 989–1005. DOI: https://doi.org/10.1193/070913EQS197M

American Lifelines Alliance (ALA) (2001). Seismic Fragility Formulations for Water Systems. American Lifelines Alliance, Washington D.C.

Baker JW (2007). Quantitative classification of near-fault ground motions using wavelet analysis. Bulletin of the Seismological Society of America, 97(5): 1486–1501. DOI: https://doi.org/10.1785/0120060255

Boore DM (2004). Estimating Vs(30) (or NEHRP site classes) from shallow velocity models (depths less than 30 m). Bulletin of the Seismological Society of America, 94(2): 591–597. DOI: https://doi.org/10.1785/0120030105

Cacciola P (2010). A stochastic approach for generating spectrum compatible fully nonstationary earthquakes. Computers and Structures, 88(15–16): 889–901. DOI: https://doi.org/10.1016/j.compstruc.2010.04.009

Cornell CA, Jalayer F, Hamburger RO, and Foutch DA (2002). Probabilistic basis for 2000 SAC Federal Emergency Management Agency steel moment frame guidelines. Journal of Structural Engineering ASCE, 128(4): 526–533. DOI: https://doi.org/10.1061/(ASCE)0733-9445(2002)128:4(526)

Darendeli MB (2001). Development of a New Family of Normalized Modulus Reduction and Material Damping Curves. Ph.D. Thesis, University of Texas at Austin, Austin, TX.

Dehghanian K (2016). A Semi-Empirical Method for Estimation of Maximum Seismic Shear Strain in Imperforated Ground Excited by Vertically Propagating Shear Waves. Ph.D. Thesis, Middle East Technical University, Ankara, Turkey.

Der Kiureghian A (1980). Structural response to stationary excitation. Journal of the Engineering Mechanics Division ASCE, 106(6): 1195–1213. DOI: https://doi.org/10.1061/JMCEA3.0002659

Federal Highway Administration (FHWA) (2004). Technical Manual for Design and Construction of Road Tunnels – Civil Elements. FHWA-NHI-09-010, U.S. Department of Transportation, Washington D.C.

Federal Highway Administration (FHWA) (2009). Technical Manual for Design and Construction of Road Tunnels – Civil Elements. FHWA-NHI-10-034, U.S. Department of Transportation, Washington D.C.

Hardin BO and Drnevich VP (1972). Shear modulus and damping in soils: design equations and curves. Journal of the Soil Mechanics and Foundations Division ASCE, 98(7): 667–692. DOI: https://doi.org/10.1061/JSFEAQ.0001760

Hashash YMA, Hook JJ, Schmidt B, and Yao JIC (2001). Seismic design and analysis of underground structures. Tunnelling and Underground Space Technology, 16(4): 247–293. DOI: https://doi.org/10.1016/S0886-7798(01)00051-7

Hashash YMA, Musgrove MI, Harmon JA, Ilhan O, Xing G, Numanoglu O, Groholski DR, Phillips CA, and Park D (2020). DEEPSOIL 7.0, User Manual. Board of Trustees of University of Illinois at Urbana-Champaign, Urbana, IL.

Hashash YMA, Park D, and Yao JIC (2010). Ovaling deformations of circular tunnels under seismic loading, an update to analytical and design criteria. Tunnelling and Underground Space Technology, 25(5): 549–560. DOI: https://doi.org/10.1016/j.tust.2010.07.004

Huang NE, Shen Z, Long SR, Wu MC, Shih HH, Zheng Q, Yen N-C, Tung CC, and Liu HH (1998). The empirical mode decomposition and the Hilbert spectrum for nonlinear and non-stationary time series analysis. Proceedings of the Royal Society A: Mathematical Physical and Engineering Sciences, 454(1971): 903–995. DOI: https://doi.org/10.1098/rspa.1998.0193

Imai T, Fumoto H, and Yokota K (1981). The relationship between N-value and shear wave velocity and shear modulus in the ground. In Proceedings of the 2nd European Symposium on Penetration Testing, Amsterdam, Netherlands, pp. 67–72.

Newmark NM (1968). Problems in wave propagation in soil and rock. In Proceedings of the International Symposium on Wave Propagation and Dynamic Properties of Earth

Materials, University of New Mexico Press, Albuquerque, NM, pp. 7–26.

Owen GN and Scholl RE (1981). Earthquake Engineering of Large Underground Structures. Report No. FHWA/RD-80/195, Federal Highway Administration, Washington D.C.

Penzien J (2000). Seismically induced racking of tunnel linings. Earthquake Engineering and Structural Dynamics, 29(5): 683–691. DOI: https://doi.org/10.1002/(SICI)1096-9845(200005)29:5<683::AID-EQE932>3.0.CO;2-1

Priestley MB (1965). Evolutionary spectra and non-stationary processes. Journal of the Royal Statistical Society Series B: Statistical Methodology, 27(2): 204–237. DOI: https://doi.org/10.1111/j.2517-6161.1965.tb01488.x

Priestley MB (1967). Power spectral analysis of non-stationary random processes. Journal of Sound and Vibration, 6(1): 86–97. DOI: https://doi.org/10.1016/0022-460X(67)90160-5

Sanchez-Sesma FJ and Campillo M (1991). Diffraction of P, SV, and Rayleigh waves by topographic features: a boundary integral formulation. Bulletin of the Seismological Society of America, 81(6): 2234–2253. DOI: https://doi.org/10.1785/BSSA0810062234

St. John CM and Zahrah TF (1987). Aseismic design of underground structures. Tunnelling and Underground Space Technology, 2(2): 165–197. DOI: https://doi.org/10.1016/0886-7798(87)90011-3

Stewart JP and Kwok AOL (2008). Nonlinear seismic ground response analysis: code usage protocols and resulting uncertainties. In Proceedings of the 4th Decennial Geotechnical Earthquake Engineering and Soil Dynamics Conference, ASCE, Sacramento, CA, pp. 1–16.

Teague DP and Cox BR (2016). Site response implications associated with using non-unique Vs profiles from surface wave inversion in comparison with other commonly used methods of accounting for Vs uncertainty. Soil Dynamics and Earthquake Engineering, 91: 87–103. DOI: https://doi.org/10.1016/j.soildyn.2016.09.034

Toro GR (1995). Probabilistic Models of Site Velocity Profiles for Generic and Site-Specific Ground-Motion Amplification Studies. Technical Report 779574, Brookhaven National Laboratory, Upton, NY.

Vanmarcke EH (1975). On the distribution of the first-passage time for normal stationary random processes. Journal of Applied Mechanics ASME, 42(1): 215–220. DOI: https://doi.org/10.1115/1.3423521

Wang JN (1993). Seismic Design of Tunnels: A State-of-the-Art Approach. Monograph 7, Parsons Brinckerhoff Inc., New York, NY.

Yoshida N, Kobayashi S, Suetomi I, and Miura K (2002). Equivalent linear method considering frequency dependent characteristics of stiffness and damping. Soil Dynamics and Earthquake Engineering, 22(3): 205–222. DOI: https://doi.org/10.1016/S0267-7261(02)00011-8

Amorosi A, Boldini D, and Elia G (2014). Parametric study on seismic ground response by finite element modelling. Computers and Geotechnics, 37(4): 515–528. DOI: https://doi.org/10.1016/j.compgeo.2010.02.009